Applied Physics Letters

Low pressure drive of the domain wall in Pt/Co/Au/Cr_2O_3/Pt thin films by the magnetoelectric effect

Cite as: Appl. Phys. Lett. **120**, 092404 (2022); https://doi.org/10.1063/5.0083202
Submitted: 22 December 2021 • Accepted: 23 February 2022 • Published Online: 04 March 2022

Jiaqi Shen, Tatsuo Tada, Kentaro Toyoki, et al.

Applied Physics Letters ARTICLE scitation.org/journal/apl

Low pressure drive of the domain wall in Pt/Co/Au/Cr_2O_3/Pt thin films by the magnetoelectric effect

Cite as: Appl. Phys. Lett. **120**, 092404 (2022); doi: 10.1063/5.0083202
Submitted: 22 December 2021 · Accepted: 23 February 2022 ·
Published Online: 4 March 2022

Jiaqi Shen,[1] Tatsuo Tada,[1] Kentaro Toyoki,[1] Yoshinori Kotani,[2] Ryoichi Nakatani,[1,3] and Yu Shiratsuchi[1,3,a)]

AFFILIATIONS

[1]Department of Materials Science and Engineering, Graduate School of Engineering, Osaka University, 2-1 Yamadaoka, Suita, Osaka 565-0871, Japan
[2]Center for Spintronics Research Network, Graduate School of Engineering Science, Osaka University, 1-3 Machikaneyama, Toyonaka 560-8351, Japan
[3]Japan Synchrotron Radiation Research Institute (JASRI/SPring-8), 1-1-1, Kouto, Sayo, Hyogo 679-5198, Japan

[a)]**Author to whom correspondence should be addressed:** shiratsuchi@mat.eng.osaka-u.ac.jps

ABSTRACT

The magnetoelectric (ME) effect is one of the methods for electrically controlling the magnetization direction. In this study, we investigated the ME-driven domain wall creep and depinning using a Pt/Co/Au/ME-Cr_2O_3/Pt thin film. The domain switching process is governed by domain wall propagation rather than the nucleation of reversed domains, similar to a pure ferromagnet. The domain wall velocity v increases exponentially with the ME pressure, that is, the simultaneous application of magnetic H and electric E fields. The v–E curve under a constant H can be scaled by the ME pressure with the assistance of the exchange bias. We determined the depinning threshold, pinning energy scale, and depinning velocity based on the model for the magnetic domain wall creep. Compared with the depinning velocity in various other systems, it was suggested that the ME-driven mechanism could yield a fast domain wall velocity utilizing the low pressure.

Magnetic materials at the nanometer scale are the key elements in spintronic/nanomagnetic devices. The key technology is the high-speed and low-energy control over the magnetization direction and/or the magnetic domain state. The application of the magnetic field H is a conventional method, and the electric current usually generates H, that is, the Oersted field.[1] This simple method is hindered by the increasing energy consumption associated with the decreasing device size, that is, the increasing integration density. Other techniques using the spin-polarized current,[2,3] spin–orbit torque,[4] and electric field E[5] are being developed to solve this problem. The magnetoelectric (ME) effect is another principle.[6,7] It is caused by the interplay between the charge and spin, namely, the dielectric polarization P induced by H or the magnetization M induced by E,[8] and emerges in some antiferromagnetic (AFM) insulators, such as Cr_2O_3[9,10] and $TbMnO_3$.[11] Symmetry arguments[12] showed that the energetic degeneration for the oppositely directed ME domains was resolved by applying E and H simultaneously. The energy difference, and thus, the driving force of the ME domain switching, is expressed by $\Delta F = 2\alpha_{ij}E_iH_j$ (α_{ij}: ME susceptibility). The expression for ΔF is analogous to the Zeeman energy of ferromagnetic (FM) materials by replacing the E-induced magnetization α_iE_i with the saturation magnetization M_S. Although the ME effect is believed to induce magnetization switching by low pressure, a quantitative comparison with other stimuli, such as H, is insufficient.

The domain wall (DW) motion is a magnetization switching process. The switching energy and speed can be quantitatively evaluated using the DW velocity v. The switching dynamics under different input pressures, that is, the H-dependence of v, is typically classified into three regimes: creep, depinning, and flow.[13] In some cases, steady flow and the so-called Walker breakdown are observed,[14] which are often masked by creep motion.[15] The steady and precessional magnetic DW flows are expressed by material-dependent parameters, such as the Gilbert damping parameter.[14,16] In contrast, the creep motion is dominated by extrinsic parameters, such as the defect-dependent depinning potential. In the creep regime, a universal law has been reported,[17] which helps to obtain the inherent v masked by the creep motion.[18] This universality has so far been confirmed for H-driven,[15,19,20] current-driven,[20] and E-driven[21] DW creep in metal ferromagnets,[15,22–27] and magnetic semiconductors.[19,20]

The creep-masked inherent v has also been evaluated for some of these materials.[18] In this study, we investigated ME-driven DW creep and depinning. The inherent v driven by the ME pressure was estimated based on the universal law and compared the obtained value with other systems.

Owing to the AFM nature of many ME materials, the detection technique usually used for the FM DW velocity is difficult to adopt. The roughness-insensitive surface magnetization in ME materials[28,29] can solve this difficulty. The surface magnetization is coupled with the AFM order parameter and, thus, the ME domain state. The surface magnetization, which manifests in the exchange bias polarity[6,30–32] or the anomalous Hall voltage,[33,34] has been experimentally proven in both bulk $Cr_2O_3(0001)$[30] and $Cr_2O_3(0001)$ thin films.[31,33] In this study, we adopted the exchange-bias technique using a Pt/Co/Au/Cr_2O_3/Pt thin film. The details of the detection scheme are available in our previous report.[7] Preliminary investigations for confirming some prerequisites that allow the application of the above detection method are summarized in the supplementary material.

A Pt(2 nm)/Co(0.4 nm)/Au(0.7 nm)/Cr_2O_3(90 nm)/Pt(20 nm) thin film was fabricated on an α-$Al_2O_3(0001)$ substrate using a DC magnetron sputtering method. This structure allows us to visualize the ME domain of the Cr_2O_3 layer via the magnetic domain of Co.[35] The Au spacer layer was used to maintain the exchange bias in the temperature regime where the ME susceptibility increased.[36] The details of the preparation method and role of the spacer layer are available in our previous studies.[36,37] Reflection high-energy electron diffraction (RHEED), x-ray reflectivity (XRR), and high-angle x-ray diffraction (XRD) measurements were performed to determine the film structure. These measurements revealed that the twinned $Cr_2O_3(0001)$ film was formed, and the interface roughness at the FM/Cr_2O_3 interface was below 0.5 nm. The structural information is provided in the supplementary material.

v was evaluated based on the change in the domain pattern with the pulsed ME pressure. The quasi-static technique, where the domain was observed at zero H and E after the pulsed ME pressure application, was adopted. The evaluation procedure is as follows.

Step 1: The domain state was initialized by applying $\mu_0 H = 5$ T. This process generated a single-domain state. Subsequently, $\mu_0 H = +3.00$ T and $E = -38.8$ MV/m (-3.5 V) were applied to create the partially reversed magnetic domain state [see Fig. 2(a)]. This process was employed to minimize the possibility of involving the nucleation of the reversed domain during the switching process, especially in the fast pulse regime. Notably, we confirmed that $\mu_0 H$ below 3 T alone did not disturb the domain state.

Step 2: Pulsed ME pressure was applied. The static H and pulsed E were superimposed. During the application of E, $\mu_0 H$ was varied as 3.00, 2.75, and 2.50 T. The pulse amplitude was varied from -33.3 MV/m (-3.0 V) to -161 MV/m (-14.5 V), while the pulse width t_{pls} was varied from 10 to 100 ns. The actual amplitude of the applied voltage was monitored using an oscilloscope. The pulsed voltage was applied after stabilizing H. Therefore, the rise time of H does not affect t_{pls}.

Step 3: The domain was observed after removing the ME pressure. The travel distance of the DW l was evaluated from the difference in the domain patterns before and after applying the ME pressure. v was calculated as the slope of the l–t_{pls} plot.

Step 4: Steps 2 and 3 were repeated until saturation. Then, the process reverted to Step 1.

The above procedure was applied to microdots of 30 μm diameter fabricated using photolithography and Ar ion milling. An optical microscope image of the device with the electric circuit is shown in Fig. 1. The positive directions of H and E were defined as the direction from the bottom electrode to the top electrode. In this experiment, H and E were applied in the positive and negative directions, respectively, so that the exchange bias assisted the switching.[38,39] The leakage current at -4.2 V was approximately 30 nA. The estimated temperature rise because of the Joule heating for $E = -150$ MV/m and $t_{pls} = 100$ ns was below mK, which was negligible. (Details are provided in the supplementary material.)

The scanning soft x-ray magnetic circular dichroism (XMCD) microscope[40] at BL25SU, SPring-8 was used for observations. The circularly polarized soft x ray was focused on the sample surface using a Fresnel zone plate (FZP) and an order-sorting aperture (OSA). The incidence direction was perpendicular to the film surface. In maintaining the focused state, the sample was scanned two dimensionally to collect the spatial mapping of the soft x-ray absorption. The XMCD images, which correspond to the magnetic domain pattern, were collected by subtracting two images for the incident soft x rays with the opposite helicity. The OSA-collection method,[41] where the emitted photoelectrons were captured by the OSA, was adopted. The photon energy of the incident soft x ray was 778.6 eV, Co L_3 edge. The observation temperature was 270 K.

Figures 2(a)–2(f) show an example of the domain evolution caused by the ME pressure. Some separated dark gray regions are observed in the initial state [Fig. 2(a)] formed in step 1. These reversed domains are observed at both the edge and inner parts of the dot, suggesting that nucleation occurs at structural inhomogeneities, such as defects and grain boundaries, rather than the demagnetization energy. The dark gray regions expand owing to the pulsed ME pressure. Further application of pulsed ME pressure sequentially changes the domain pattern. As shown in Figs. 2(b)–2(f), the DW edge expands concentrically, suggesting that the DW propagation governs the switching. A small number of nucleated domains, which are indicated by the yellow arrow, are observed for $t_{pls} = 10$–30 ns [Figs. 2(b)–2(d)]. These domains were excluded for the analysis of v. Small gray dots [white arrow in Figs. 2(b)–2(d)] do not expand by the application of ME pressure. The contrast may be due to the artifact. Iyama and Kimura reported that at finite H, Cr_2O_3 behaved as ferroelectric.[42] The Kolmogorov–Avrami–Ishibashi model[43,44] for pure FE materials predicts the initiation of switching by the nucleation of small domains. The domains first grow along the vertical direction (forward growth)

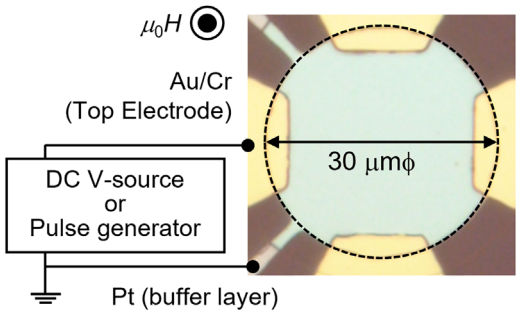

FIG. 1. Optical microscope image of the fabricated device with the electrical circuit.

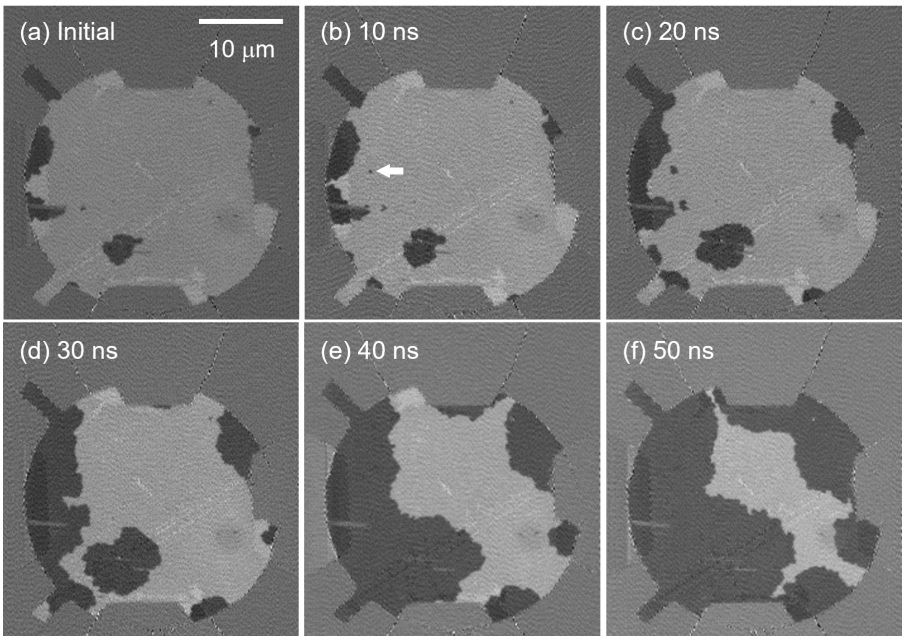

FIG. 2. Representative series of magnetic domain images after applying ME pressure. $\mu_0 H$ and E for images (a)–(f) are 2.75 T and −139 MV/m (12.5 V), respectively. (a) depicts an initial state. t_{pls} for each image is (b) 10, (c) 20, (d) 30, (e) 40, and (f) 50 ns. The light and dark regions correspond to the regions where the Co moment is directed downwards and upwards, respectively. Yellow and white arrows in (b)–(d) indicate the newly nucleated domains and the artefactual contrast by defects, respectively.

until they penetrate the film, followed by growth in the lateral direction. Hence, the penetrated domains from the bottom side are observed before lateral growth. The so-called back switching, where the nucleated reversed domains vanish again upon removal of the field, sometimes occurs in the FE film.[45] Since our quasi-static method cannot capture this process, we do not claim its absence. In contrast, a similar switching process dominated by DW propagation is usually observed in pure FM materials. Therefore, the switching process in the film may be dominated by the magnetic origin because the surface magnetization dominates the switching dynamics.[46,47] The difference in FM and FE origins would manifest in the difference in the critical exponents of the DW creep. Herein, we focus on the depinning behavior, and the detailed analysis of the critical exponent in the low-pressure regime would be performed in future studies.

The typical change in l with t_{pls} is shown in the inset of Fig. 3(a). The mean DW velocity v_{mean} can be estimated using the linear relationship between l and t_{pls}, which is true for every ME condition. The main figure in Fig. 3(a) shows that v_{mean} increases with E. A similar relationship was observed for the different values of $\mu_0 H$. The curve shifts toward high E as $\mu_0 H$ decreases because the driving force for the DW motion is lowered. In our experimental condition, the exchange bias assists the switching, and the total driving force of the DW motion is given by[47]

$$F = 2\alpha EH + F_{EB}, \tag{1}$$

$$F_{EB} = \frac{J_K}{t_{AFM}}. \tag{2}$$

Here, α is the ME susceptibility, F_{EB} denotes the pressure caused by the exchange bias, J_K is the exchange anisotropy energy density, and

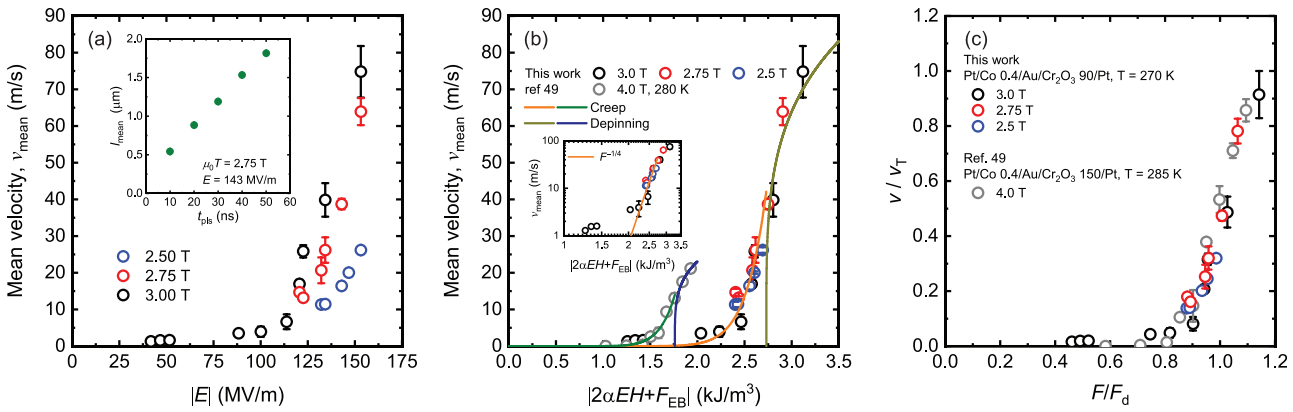

FIG. 3. Change of v_{mean} as a function of (a) E and (b) ME pressure, $2\alpha EH + F_{EB}$. In (b), the data for Pt(1.5)/Co(0.4)/Au(1.0)/Cr_2O_3(150)/Pt(20) from Ref. 49 is also shown. The lines represent the fitted results by Eq. (4). Inset shows the log v_{mean}–log F plot with the relationship of $v_{mean} \propto F^{-1/4}$ (orange line). (c) Normalized v–F curve by the depinning velocity vT and the depinning pressure F_d. The inset of (a) represents the change in the mean DW displacement as a function of t_{pls} for $\mu_0 H = 2.75$ T and $E = -143$ MV/m.

t_{AFM} is the AFM layer thickness. J_K can be evaluated from the magnetization curve for the FM layer and is expressed as follows:

$$J_K = H_{EB} \cdot M_S \cdot t_{FM}, \tag{3}$$

where H_{EB} is the exchange bias field, M_S is the saturation magnetization of the FM layer, and t_{FM} is the FM layer thickness. The estimations of $\mu_0 H_{EB}$ and M_S are presented in the supplementary material. α is assumed to be 3.5 ps/m based on the reported value for the bulk Cr_2O_3.[48] In Fig. 3(b), v is re-plotted as a function of F. The three v–F curves coincide with each other. The highest value of v was approximately 77 m/s at $F = 3\,\mathrm{kJ/m^3}$.

For a more quantitative discussion, the obtained v–F curve is analyzed based on the universal law of the magnetic DW creep expressed as[18]

$$v(F,T) = v(F_d,T)\exp\left[-\frac{T_d}{T}\left\{\left(\frac{F_d}{F}\right)^{0.25} - 1\right\}\right], \tag{4a}$$

$$v(F_d,T) \sim v_T(F_d,T)\left(\frac{T}{T_d}\right)^{0.15},$$

$$v(F,T) \sim \frac{v_T(F_d,T)}{0.65}\left(\frac{F-F_d}{F_d}\right)^{0.25}, \tag{4b}$$

where $F_d = (2\alpha_{ij}E_iH_j + F_{EB})_d$ denotes the depinning pressure, T_d is the depinning temperature, and v_T is the depinning velocity. Eq. (4a) is a modified form of the simple exponential function that covers the thermally assisted flux flow (TAFF) regime based on empirical law. The solid lines in Fig. 3(b) demonstrate that the experimental data are well reproduced by the universal law of the DW creep. We also re-analyzed the results presented in Ref. 49, which were also reproduced by the same model. The parameters used for the calculations are listed in Table I. Figure 3(c) shows the reduced v–F curve. The v–F curves collected for the different conditions, such as E, H, T, t_{AFM}, and J_K, are merged into a single curve, indicating the validity of the universal depinning behavior for the ME-induced mechanism. To elucidate more details on the creep motion, such as the critical exponent, more data points are required in the low-pressure regime, e.g., $<1.5\,\mathrm{kJ/m^3}$. However, the relationship $v_{mean} \propto (2\alpha EH + F_{EB})^{-1/4}$ was confirmed [as shown in Fig. 3(b)] in the depinning regime. The roughness exponent (ζ) of the DW was approximately 0.69, which was similar to the previously reported value[13] and the theoretically predicted value for one-dimensional DW,[17] coinciding with the critical exponent used in Eq. (4a). The details of ζ are presented in the supplementary material.

v_T is recognized as a DW flow velocity in the absence of pinning, and it is expected to be a material-dependent parameter.[18] Here, we compare the obtained v_T with other magnetic systems, wherein the DW motion is driven by H alone. Figure 4 shows a map of v_T as a function of F_d where M_SH_d was used as the depinning pressure for the FM films because the ME pressure is equivalent to the Zeeman energy, as mentioned above. In general, v_T increases with F_d. This trend originates from the similar DW mobility, m_{fl} (= v_{flw}/H). Although v_T for the ME-induced mechanism is similar to that of Pt/Co/Pt[15,25,27] and Au/Co/Au[22] systems, the depinning pressure is 1–2 orders lower. In comparison with the (Ga, Mn)(As, P) films,[20] both v_T and depinning pressure are approximately one order of magnitude higher. The low depinning pressure in an ME-mechanism is due to the small magnitude of the E-induced magnetic moment. The direct comparison of v_T with pure FE materials is difficult because a similar analysis has not been performed for the FE DW motion. Nonetheless, the depinning pressure of the FE DW, P_SE_0 (P_S: the saturation polarization, E_0: the depinning E) is typically above $10^6\,\mathrm{J/m^3}$, and the FE DW velocity at the depinning condition is below 10^{-1} m/s.[50–53] These values are approximately three orders higher and one to two orders slower than the ME case, respectively. It is also likely that $\sim$10 MJ/m^3, an approximately three-order high pressure is required to obtain a similar DW velocity of $\sim$40 m/s for the 400-nm-thick $Pb(Zr_{0.45}Ti_{0.55})O_3$ thin film.[54]

Finally, we compared the estimated v_T with the theoretically predicted value. In the steady state driven by the ME pressure, v can be expressed as[46]

$$v = \frac{2\varepsilon/\alpha_0}{1+(\varepsilon/\alpha_0)^2}\frac{\gamma\mu_0 H\lambda}{2}, \tag{5}$$

where $\varepsilon = \alpha E/L$, $\boldsymbol{L} = (\boldsymbol{M}_1 - \boldsymbol{M}_2)/2$ is the AFM order parameter (staggered magnetization), $\boldsymbol{M}_1$ and $\boldsymbol{M}_2$ are the sublattice magnetization, α_0

TABLE I. Parameters describing the magnetic DW creep obtained from Fig. 3(b). Some measurement parameters are also listed.

Parameter	This work	Ref. 48
Measurement T (K)	270	285
t_{AFM} (nm)	90	150
$\mu_0 H_{EB}$ (mT)	74	54
J_K (mJ/m^2)	0.050	0.035
F_{EB} (J/m^3)	560	230
α (ps/m) (Ref. 48)	3.5	2.0
T_d (K)	1.3×10^4	1.2×10^4
F_d (kJ/m^3)	2.7	1.8
$v(F_d, T)$ (m/s)	42	14
v_T (m/s)	76	25

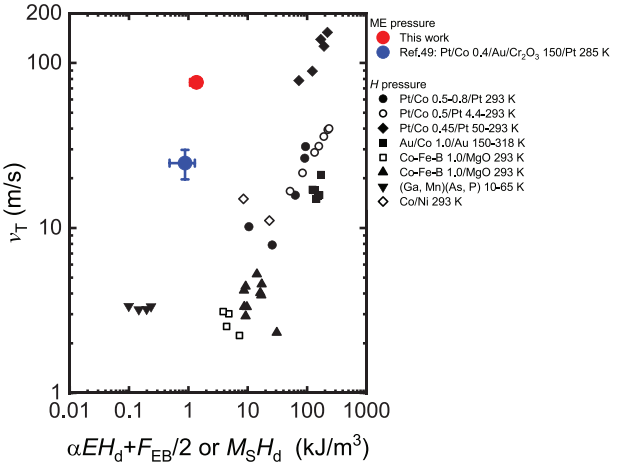

FIG. 4. Map of v_T as a function of the depinning pressure with various data from Ref. 18.

is the damping parameter, γ is the gyromagnetic factor, and λ is the DW width. Equation (5) shows that the maximum velocity (v_{max}) is obtained at $\varepsilon = \alpha_0$, and v gradually decreases with an increase in ε. This is reminiscent of the Walker breakdown of the pure FM case.[14] That is, the DW flow for ε below and above α_0 corresponds to the steady flow and the precessional flow, respectively. Assuming L and α for the bulk Cr_2O_3[47] and α_0 for the predicted value,[46] for v_{max}, E is estimated to be 32 MV/m. This value is lower than the obtained depinning E (~100 MV/m). Therefore, the estimated v_T was attributed to that of the precessional flow.

Finally, the influence of the FM layer using the ratio of v_T is discussed. Using Eq. (5), v at $E = 125$ MV/m and $\mu_0 H = 3$ T, that is, near the depinning condition is estimated to be approximately 600 m/s. The expected value was approximately eight times higher than our results. This significant difference may be attributed to the enhanced damping parameter owing to spin–orbit coupling,[55] and/or the spin pumping effect.[56,57] The exchange coupling with the FM layer induces the enhancement of the effective damping parameter.[49] The detection of surface magnetization without using interfacial exchange coupling is beneficial for avoiding this effect. This may be achieved by employing an FM layer-free device, such as Pt/Cr_2O_3, with the emergence of the remanent anomalous Hall effect,[33,34] which is now under investigation.

In summary, we investigated the creep and depinning of DW under ME pressure. In this study, we employed the exchange bias technique to detect ME-controlled surface magnetization. The switching process was dominated by DW propagation, and the nucleation of reversed domains was rarely observed. This switching process is similar to that of pure FM films, rather than pure FE films. v increased with the ME pressure and could be scaled by $F = \alpha EH + F_{EB}/2$. Based on the theory of magnetic DW creep and depinning, several parameters, such as F_d and v_T, were estimated. Compared to various perpendicular magnetic thin films, a high v_T could be achieved at a low depinning pressure because of the small magnitude of the E-induced magnetic moment. The obtained v_T was significantly lower than the theoretically expected value. Further investigations, for example, using the FM-free device, may provide deeper insight into the possible fast DW dynamics of ME materials.

See the supplementary material for the structural information, prerequisites of the detection, electric property, and the roughness parameter of DW.

XMCD measurements were performed with the approval of JASRI (Project Nos. 2017B0079, 2018A1353, 2018B1338, 2018B1384, 2019A1200 2019B1196, 2020A1172, 2021A1228, and 2021B1206). This work was partly supported by JSPS KAKENHI (Project No. 19H00825).

AUTHOR DECLARATIONS

Conflict of Interest

The authors have no conflicts to disclose.

DATA AVAILABILITY

The data that support the findings of this study are available from the corresponding author upon reasonable request.

REFERENCES

[1]S. Ikegawa, F. B. Mancoff, J. Janesky, and S. Sggarwal, IEEE Trans. Electron Device **67**, 1407 (2020).
[2]J. C. Slonczeski, J. Magn. Magn. Mater. **159**, L1 (1996).
[3]L. Berger, Phys. Rev. B **54**, 9353 (1996).
[4]I. M. Miron, K. Garello, G. Gaudin, P.-J. Zermatten, M. V. Costache, S. Auffret, S. Bandiera, B. Rodmaq, A. Schuhl, and P. Gambardella, Nature **476**, 189 (2011).
[5]T. Maruyama, Y. Shiota, T. Nozaki, K. Ohta, N. Toda, M. Mizuguchi, A. A. Tulapurkar, T. Shinjo, M. Shiraishi, S. Muzukami, Y. Ando, and Y. Suzuki, Nat. Nanotechnol. **4**, 158 (2009).
[6]P. Borisov, A. Hochstrat, X. Chen, W. Kleemann, and C. Binek, Phys. Rev. Lett. **94**, 117203 (2005).
[7]Y. Shiratsuchi, K. Toyoki, and R. Nakatani, J. Phys.: Condens. Matter **33**, 243001 (2021).
[8]M. Fiebig, J. Phys. D **38**, R123 (2005).
[9]I. E. Dzyaloshinskii, J. Exptl. Theoret. Phys. (U.S.S.R) **37**, 881 (1959).
[10]D. N. Astorov, J. Exptl. Theoret. Phys. (U.S.S.R.) **38**, 984 (1960).
[11]T. Kimura, T. Goto, H. Shintani, K. Ishizaka, T. Arima, and Y. Tokura, Nature **426**, 55 (2003).
[12]T. J. Martin and J. C. Anderson, IEEE Trans. Magn. **2**, 446 (1966).
[13]S. Lemerle, J. Ferre, C. Chappert, V. Mathet, T. Giamarchi, and P. Le Doussal, Phys. Rev. Lett. **80**, 849 (1998).
[14]G. S. D. Beach, C. Nitor, C. Knutson, M. Tsoi, and J. L. Erskine, Nat. Mater. **4**, 741 (2005).
[15]P. J. Mataxas, J. P. Jamet, A. Mougin, M. Cormier, J. Ferré, V. Baltz, B. Rodmaq, B. Dieny, and R. L. Stamps, Phys. Rev. Lett. **99**, 217208 (2007).
[16]T. Ono, H. Miyajima, K. Shigeto, K. Mibu, N. Hosoito, and T. Shinjo, Science **284**, 468 (1999).
[17]P. Chauve, T. Giamarchi, and P. Le Doussal, Phys. Rev. B **62**, 6241 (2000).
[18]V. Jeudy, R. D. Pardo, W. S. Torres, S. Bustingorry, and A. B. Kolton, Phys. Rev. B **98**, 054406 (2018).
[19]V. Jeudy, A. Mougin, S. Bustingorry, W. S. Torres, J. Gorchon, A. B. Kolton, A. Lemaître, and J.-P. Jamet, Phys. Rev. Lett. **117**, 057201 (2016).
[20]M. Yamanouchi, J. Ieda, F. Matsukura, S. E. Barnes, S. Maekawa, and H. Ohno, Science **317**, 1726 (2007).
[21]W. Lin, N. Vernier, G. Agnus, K. Garcia, B. Ocker, W. Zhao, E. E. Fullerton, and D. Ravelosona, Nat. Commun. **7**, 13532 (2016).
[22]A. Kiriluk, J. Ferré, V. Grolier, J. P. Jamet, and D. Renard, J. Magn. Magn. Mater. **171**, 45–63 (1997).
[23]K. Yamada, J.-P. Jamet, Y. Nakatani, A. Mougin, A. Thiaville, T. Ono, and J. Ferré, Appl. Phys. Express **4**, 113001 (2011).
[24]C. Burrowes, N. Vernier, J.-P. Adam, L. H. Diaz, K. Garcia, I. Barisic, G. Agnus, S. Eimer, J.-V. Kim, T. Devolder, A. Lamperti, R. Mantovan, B. Ockert, E. E. Fullerton, and D. Ravelosona, Appl. Phys. Lett. **103**, 182401 (2013).
[25]J. Gorchon, S. Bustingorry, J. Ferré, V. Jeudy, A. B. Kolton, and T. Giamrchi, Phys. Rev. Lett. **113**, 027205 (2014).
[26]S. L. Gall, N. Vernier, F. Montaigne, M. Gottwald, D. Lacour, M. Hehn, D. Ravelosona, S. Mangin, S. Andrieu, and T. Hauet, Appl. Phys. Lett. **106**, 062406 (2015).
[27]R. D. Pardo, W. S. Torres, A. B. Kolton, S. Bustingorry, and V. Jeudy, Phys. Rev. B **95**, 184434 (2017).
[28]A. F. Andreev, JETP Lett. **63**, 758 (1996).
[29]K. D. Belashchenko, Phys. Rev. Lett. **105**, 147204 (2010).
[30]X. He, Y. Wang, N. Wu, A. N. Caruso, E. Vescovo, K. D. Belashchenko, P. A. Dowben, and C. Binek, Nat. Mater. **9**, 579 (2010).
[31]K. Toyoki, Y. Shiratsuchi, T. Nakamura, C. Mitsumata, S. Harimoto, Y. Takechi, T. Nishimura, H. Nomura, and R. Nakatani, Appl. Phys. Express **7**, 114201 (2014).
[32]T. Ashida, M. Oida, N. Shimomura, T. Nozaki, T. Shibata, and M. Sahashi, Appl. Phys. Lett. **104**, 152409 (2014).
[33]T. Kosub, M. Kopte, O. G. Schmidt, and D. Makarov, Phys. Rev. Lett. **115**, 097201 (2015).
[34]X. Wang, K. Toyoki, R. Nakatani, and Y. Shiratsuchi, "Magnetic-field and temperature dependence of anomalous Hall effect in $Pt/Cr_2O_3/Pt$ trilayer," AIP Adv. (to be published).

[35]Y. Shiratsuchi, S. Watanabe, H. Yoshida, N. Kishida, R. Nakatani, T. Kotani, K. Toyoki, and T. Nakamura, Appl. Phys. Lett. **113**, 242404 (2018).
[36]Y. Shiratsuchi, W. Kuroda, T. V. A. Nguyen, Y. Kotani, K. Toyoki, T. Nakamura, M. Suzuki, K. Nakamura, and R. Nakatani, J. Appl. Phys. **121**, 073902 (2017).
[37]Y. Shiratsuchi, T. Fujita, H. Noutomi, H. Oikawa, and R. Nakatani, IEEE Trans. Magn. **47**, 3909 (2011).
[38]T. V. A. Nguyen, Y. Shiratsuchi, A. Kobane, S. Yoshida, and R. Nakatani, J. Appl. Phys. **122**, 073905 (2017).
[39]T. V. A. Nguyen, Y. Shiratsuchi, S. Yonemura, T. Shibata, and R. Nakatani, J. Appl. Phys. **124**, 233902 (2018).
[40]Y. Kotani, Y. Semba, K. Toyoki, D. Billington, H. Okazaki, A. Yasui, W. Ueno, H. Ohashi, S. Hirosawa, Y. Shiratsuchi, and T. Nakamura, J. Synchrotron Radiat. **25**, 1444 (2018).
[41]H. Suto, N. Kikuchi, S. Okamoto, K. Toyoki, Y. Kotani, and T. Nakamura, Appl. Phys. Express **13**, 043002 (2020).
[42]A. Iyama and T. Kimura, Phys. Rev. B **87**, 180408(R) (2013).
[43]M. Avrami, J. Phys. Chem. Phys. **8**, 212 (1940).
[44]Y. Ishibashi and Y. Takagi, J. Phys. Soc. Jpn. **31**, 506 (1971).
[45]S. Kim, V. Gopalan, K. Kitamura, and Y. Furukawa, J. Appl. Phys. **90**, 2949 (2001).
[46]K. D. Belashchenko, O. Tchernyshyov, A. A. Kovaley, and O. A. Tretiakov, Appl. Phys. Lett. **108**, 132403 (2016).
[47]A. Parthasarathy and S. Rakheja, Phys. Rev. Appl. **11**, 034051 (2019).
[48]P. Borisov, T. Ashida, T. Nozaki, M. Sahashi, and D. Lederman, Phys. Rev. B **93**, 174415 (2016).
[49]Y. Shiratsuchi, H. Yoshida, Y. Kotani, K. Toyoki, T. V. A. Nguyen, T. Nakamura, and R. Nakatani, APL Mater. **6**, 121104 (2018).
[50]L. Tian, D. A. Scrymgeour, and V. Gopalan, J. Appl. Phys. **97**, 114111 (2005).
[51]J. Y. Jo, S. M. Yang, T. H. Kim, H. N. Lett, J.-G. Yoon, S. Park, Y. Jo, M. H. Jung, and T. W. Noh, Phys. Rev. Lett. **102**, 045701 (2009).
[52]L. J. McGilly, P. Yudin, L. Fiegl, A. K. Tagantsev, and N. Setter, Nat. Nanotechnol. **10**, 145 (2015).
[53]S. Answer and L. Asadi, ACS Macro Lett. **8**, 525 (2019).
[54]A. Grigoriev, D. Do, D. M. Kim, C. Eom, B. Adams, E. M. Dufresne, and P. G. Evans, Phys. Rev. Lett. **96**, 187601 (2006).
[55]V. Kambersky, Czech. J. Phys. B **26**, 1366 (1976).
[56]H.-S. Song, K.-D. Lee, J.-W. Sohn, S.-H. Yang, S. S. P. Parkin, C.-Y. You, and S.-C. Shin, Appl. Phys. Lett. **103**, 022406 (2013).
[57]T. Moriyama, K. Hayashi, K. Yamada, M. Shima, Y. Ohya, Y. Tserkovnyak, and T. Ono, Phys. Rev. B **101**, 06402(R) (2020).